

Original Article

# Histopathological significance of microRNA-210 expression in acute peripheral ischemia in a murine femoral artery ligation model

Yuichi Takai<sup>1\*</sup>, Satoshi Nishimura<sup>2</sup>, Hitoshi Kandori<sup>1</sup>, and Takeshi Watanabe<sup>1</sup>

<sup>1</sup> Drug Safety Research and Evaluation, Takeda Pharmaceutical Company Ltd., 26-1 Muraoka-Higashi 2 Chome, Fujisawa, Kanagawa 251-8555, Japan

<sup>2</sup> Cardiovascular and Metabolic Drug Discovery Unit, Pharmaceutical Research Division, Takeda Pharmaceutical Company Ltd., 26-1 Muraoka-Higashi 2 Chome, Fujisawa, Kanagawa 251-8555, Japan

**Abstract:** Under hypoxic conditions, microRNA-210 is upregulated and plays multiple physiological roles including in cell growth arrest, stem cell survival, repression of mitochondrial respiration, angiogenesis, and arrest of DNA repair. In this study, we investigated the histopathological expression of microRNA-210 under hypoxic conditions using a femoral artery ligation model established in C57BL/6J mice to determine the pathological significance of microRNA-210. Following femoral artery ligation, ischemia was represented by decreased blood flow compared to the control, in which a sham operation was performed. On histopathology, degeneration/necrosis of the muscle fibers, inflammatory cell infiltration, and regeneration of the muscle fibers were sequentially observed from 3 h to 3 d after ligation of the artery. The degree of these effects was more severe in the area in which type I muscular fibers are dominant. The histological expression of hypoxia-inducible factor 1 $\alpha$ , a well-known biomarker of hypoxia, and microRNA-210 was observed in a few necrotic muscle fibers, macrophages, and myoblasts, a distribution consistent with the histopathological lesions, and their signal increased over time. The expression of microRNA-210 in macrophages and myoblasts under ischemia might be indicative of a significant role in the recovery from ischemic lesions. In addition, the *in situ* hybridization of microRNA-210 could potentially be used for the detection of hypoxia as a histological marker in addition to the immunohistochemistry of hypoxia-inducible factor 1 $\alpha$ . (DOI: 10.1293/tox.2020-0023; J Toxicol Pathol 2020; 33: 211–217)

**Key words:** microRNA-210, hypoxia inducible factor 1, ischemia, mice

## Introduction

The expression of hypoxia inducible factors (HIFs) is upregulated under hypoxic conditions, and HIF-1 $\alpha$  is well known as an immunohistochemical biomarker for the detection of hypoxia<sup>1, 2</sup>. HIF-1 $\alpha$  is synthesized continuously but is rapidly degraded by the ubiquitin-proteasome system under normal oxygen partial pressure. Under hypoxic conditions, however, the degradation is slowed and HIF-1 $\alpha$  acts as a transcriptional factor after transferring to the nucleus and shaping heterodimers with HIF-1 $\beta$ <sup>3</sup>. HIFs control the cellular response to hypoxia by regulating genes that are involved in metabolism, angiogenesis, erythropoiesis, cell proliferation, differentiation, and apoptosis<sup>1</sup>. However, HIF-1 $\alpha$  is expressed immunohistochemically in various organs even under normal oxygen partial pressure<sup>2</sup>, which may

make it difficult to detect hypoxia using its immunohistochemistry (IHC).

Through the expression of HIF, several microRNAs (miRs) are upregulated, and miR-210 is one of the major hypoxia-inducible miRs<sup>1</sup>. miR-210 is reported to be highly expressed under hypoxic conditions such as those found in the cardiovascular system<sup>4</sup>, brain<sup>5</sup>, skin<sup>6, 7</sup>, and tumor tissue<sup>1</sup>, and plays several physiological roles including cell growth arrest, stem cell survival, repression of mitochondrial respiration, angiogenesis, and arrest of DNA repair<sup>1</sup>. However, there is no detailed description of the histopathological distribution of miR-210 under hypoxic conditions in reported in the literature.

In this study, we conducted *in situ* hybridization (ISH) of miR-210 in the skeletal muscle under ischemia using a femoral artery ligation model, and evaluated its pathological significance and usefulness as a novel histological biomarker for the detection of hypoxia.

## Materials and Methods

Seventeen-week-old male C57BL/6J mice purchased from CLEA Japan (Tokyo, Japan) were used in this study. Nine animals were maintained on a laboratory chow diet (CE-2, CLEA Japan) and allowed free access to water and

Received: 10 April 2020, Accepted: 27 April 2020

Published online in J-STAGE: 17 May 2020

\*Corresponding author: Y Takai (e-mail: yuichi.takai@takeda.com)

©2020 The Japanese Society of Toxicologic Pathology

This is an open-access article distributed under the terms of the Creative Commons Attribution Non-Commercial No Derivatives

(by-nc-nd) License. (CC-BY-NC-ND 4.0: <https://creativecommons.org/licenses/by-nc-nd/4.0/>).



food before and during the experiments. The care and use of the animals and the experimental protocols used in this research were approved by the Institutional Animal Care and Use Committee of Takeda Pharmaceutical Co., Ltd. (Approval code: 00006136).

#### *Surgical procedures and blood flow measurement*

All surgical procedures were performed under isoflurane anesthesia (1–5%) and buprenorphine analgesia (0.5–1 mg/kg, s.c.), and all efforts were made to minimize suffering. After skin incision, the proximal and distal ends of the femoral artery of the left leg were ligated. The intervening segments were excised, and the dissected sites were sutured with sterile threads. As a sham operation for the right leg, the same surgical procedure was performed except for the ligation and excision of the artery. Blood flow was measured for both lower plantar surfaces using a MoorLDI2-2λsim laser Doppler imaging system (Moor Instruments, Axminster, UK) at 3 h, 1 d, and 3 d after the surgery (3 mice each) under anesthesia by inhalation of isoflurane. As the index of blood flow, the perfusion unit, which was calculated by multiplying the number and velocity of red blood cells, was used.

#### *Pathological examination*

The animals were euthanized after each blood flow measurement by exsanguination under isoflurane anesthesia. After the necropsy, the gastrocnemius and soleus muscles were removed, trimmed and fixed in 10% (v/v) neutral buffered formalin (NBF). Portions of the gastrocnemius and soleus muscles were also immersed in RNAlater (Ambion, Inc., Austin, USA) for 24 h in a refrigerator (soleus: immersed in RNAlater after 1 h formalin fixation for better histopathological evaluation) and preserved at –80°C until quantitative polymerase chain reaction (qPCR) analysis was performed. After approximately 7 h of fixation in NBF, soleus and gastrocnemius muscles were embedded in paraffin, sectioned transversely, and stained with hematoxylin and eosin (H&E). With sequential sections of H&E, IHC for slow troponin I, sarcoplasmic/endoplasmic reticulum calcium ATPase 2 (SERCA2), and HIF-1α, and ISH for miR-210, were conducted for the characterization of muscular lesions. Details of the staining conditions for each primary antibody are summarized in Table 1. ISH was conducted according to the instruction manual v3.0 of the miRCURY LNA™ microRNA ISH Optimization Kit (FFPE), developed by Exiqon (Vedbaek, Denmark), with minor modifi-

cations. We used digoxigenin (DIG)-labeled locked nucleic acid (LNA)-modified probes for miR-210 (hsa-miR-210 Product. No. 18103-15; target sequence: CUGUGCGUGUGACAGCGGUGA, probe sequence: CAGCCGCTGTCACACGCACA), positive control (U6 snRNA, Product. No. 90010), and negative control (scrambled microRNA, Product No. 90010) from Exiqon (Vedbaek, Denmark). Following the deparaffinization process, proteinase-K (Exiqon: Product No. 90010, miRCURY LNA; microRNA Detection, control probes, buffer and ProtK) at 2 μg/ml was treated at 37°C for 10 min. After a PBS wash, the sections were dehydrated through increasing gradients of ethanol and air-dried. The LNA-probes were denatured by heating to 90°C for 4 min. Hybridization of the LNA-probes miR-210 (200 nM), scramble-miR (40 nM), and U6 (1 nM) was carried out at 60°C for 60 min. After immersion in 5× SSC buffer at room temperature, specimens were washed in pre-heated SSC buffers (55°C), 1× 5 min in 5× SSC, 2× 5 min in 1× SSC, 2× 5 min in 0.2× SSC, and finally 1× 5 min 0.2× SSC at room temperature and then immersed in PBS. Sections were blocked against unspecific binding in blocking solution composed of 2% (v/v) sheep serum and 1% (v/v) BSA in PBS-T for 15 min at room temperature. Alkaline phosphatase (AP)-conjugated anti-DIG (Product No. 1093274, Roche, Mannheim, Germany) 1:800 was incubated for 60 min at room temperature for immunologic detection. After a PBS-T wash, the substrate enzyme reaction was carried out with NBT/BCIP (Product No. 1697471, Roche) at 30°C for 120 min. The reaction was stopped with a 2× 5 min wash in KTBT buffer (50 mM Tris-HCl, 150 mM NaCl, 10 mM KCl). Sections were counter-stained with Nuclear Fast Red at room temperature for 1 min and then rinsed in tap water. After dehydration by increasing gradients of ethanol solutions, specimens were mounted with Permount (Fisher Scientific Inc., Pittsburgh, PA, USA).

#### *miRNA quantification*

For relative quantification of miR-210, qPCR was conducted after extraction of total miRNA and reverse transcription to cDNA. Using cryopreserved muscle samples, total miRNA was extracted using miRNeasy Mini Kit (Product No. 217004, QIAGEN, Hilden, Germany) for the gastrocnemius and miRNeasy FFPE Kit (Product No. 217504, QIAGEN) for the soleus according to the kit protocol, with the exception that a tissue homogenization process was used instead of deparaffinization for the soleus. Reverse

**Table 1.** Primary Antibodies and Reaction Conditions for Immunohistochemistry

| Antibody         | Host   | Clonality   | Supplier               | Dilution | Antigen retrieval    | Detection system             |
|------------------|--------|-------------|------------------------|----------|----------------------|------------------------------|
| Slow Troponin -I | Mouse  | mono        | Kanto<br>(01869-96)    | ×100     | AC, 121°C, 15 min    | Histofine®<br>MOUSESTAIN KIT |
| SERCA2           | Rabbit | poly        | Abcam<br>(ab3625)      | ×2,000   | Trypsin 37°C, 30 min | Envision+ HRP, Rabbit        |
| HIF-1α           | Mouse  | mono: H1α67 | Calbiochem<br>(400080) | ×500     | AC, 121°C, 10 min    | Histofine®<br>MOUSESTAIN KIT |

AC: autoclave, immersed in citric buffer (pH6); mono: monoclonal; poly: polyclonal; SERCA2: sarcoplasmic/endoplasmic reticulum calcium ATPase 2; HIF-1α: hypoxia inducible factor-1α.

transcription to cDNA was conducted with the Universal cDNA Synthesis Kit II (Product No. 203301, Exiqon, Vedbaek, Denmark). Thereafter, miR-210 levels (hsa-miR-210, Product No. 204333; target sequence: CUGUGCGUGUGA-CAGCGGCUGA, Exiqon) relative to miR-191-5p, as an endogenous control (has-miR-191-5p, Product No. 204306, Exiqon), were analyzed using ExiLent SYBR Green master mix (Product No. 203402, Exiqon) with the 7900 HT Fast Real Time PCR System (Applied Biosystems, Foster City, CA, USA).

### Statistical analysis

Blood flow and qPCR data were tested using the F-test for homogeneity of variance between ischemic and non-ischemic hindlimbs. When the variances were homogeneous, the Student's *t*-test was used, and when the variances were heterogeneous, the Aspin & Welch *t*-test was performed to compare the mean of the control group with that of the dosage group<sup>8</sup>. The F-test was conducted at the significance level of 0.20, and the other tests were conducted at the two-tailed significance levels of 0.05 and 0.01. All statistical analysis was performed using SAS version 9.3 (SAS Institute Inc., Cary, NC, USA).

## Results

### Blood flow measurement

To characterize the degree of ischemia following femoral artery ligation, blood flow at the plantar surface of both hindlimbs was measured by laser Doppler perfusion imaging. Compared with the non-ischemic hindlimb, a reduction in blood flow was noted at 3 h, 1 d, and 3 d after the ischemic surgery with blood flow ratios (ischemia/sham) of 9%, 10%, and 15%, respectively (Table 2), which confirmed the continuous ischemic condition through the experiment period.

### Histopathology

In the soleus, necrosis/degeneration of muscle fibers was noted in more than half of the area in the ischemic hindlimb from 3 h. Infiltration of neutrophils and macrophages were observed in the interstitial tissue consistent with the necrotic area from 1 d after ligation, and regeneration of the muscle fiber with the sporadic appearance of myoblasts was observed at 3 d after ligation (Fig. 1). Similar lesions were also noted in the gastrocnemius, although to a lesser severity than those in the soleus.

### IHC and ISH

SERCA2 and slow troponin I: In the non-ischemic hindlimb, one third of muscle fibers in the soleus and only a few fibers in the gastrocnemius showed positive for SERCA2 and slow troponin I, the histological marker of type I muscle fiber (Fig. 2). This distribution in the ischemic hindlimbs was comparable to the non-ischemic hindlimbs (sham) (Fig. 2) from 3 h to 3 d after the artery ligation, and positive fibers in the gastrocnemius were mainly noted in the necrotic/degenerative area.

HIF-1 $\alpha$  and miR-210: Positive HIF-1 $\alpha$  and miR-210 signals were not noted in the non-ischemic muscle tissue. In the ischemic hindlimbs, a few necrotic muscle fibers and infiltrative cells showed positive for HIF-1 $\alpha$  and miR-210 at 3 h and 1 d after the artery ligation. No positive results were observed in the intact muscle fibers in the ischemic hindlimb. The magnitude of the positive signal was prominent in macrophages and regenerative myoblasts at 3 d, consistent with the distribution of the ischemic histopathology. The positive signals of HIF-1 $\alpha$  and miR-210 were mainly located in the cytoplasm, and that of HIF-1 $\alpha$  was also noted in a few nuclei in the myoblasts. Histological distributions were comparable between HIF-1 $\alpha$  and miR-210 in the ischemic lesion (Fig. 3 and 4).

### Relative quantification of miR-210

Although statistically significant changes were not observed, the expression of miR-210 in ischemic hindlimbs tended to be higher than in non-ischemic hindlimbs at 3 d after ligation in the soleus, and at 1 and 3 d after ligation in the gastrocnemius (Table 3).

## Discussion

MiR-210 is highly expressed under hypoxic conditions<sup>1</sup>. It could aid in tissue repair under hypoxic conditions through angiogenesis and proliferation of fibroblasts<sup>9–12</sup>. Furthermore, miR-210 may have protective effects on skeletal muscle and cardiac tissue under ischemic conditions through the inhibition of reactive oxygen species formation by switching from phosphorylation to glycolysis or by regulating apoptosis<sup>13, 14</sup>. However, there has been no detailed description of miR-210 histopathological distribution under hypoxic conditions in previous research. We therefore examined the histopathological distribution of miR-210 in a mouse model under hypoxic conditions.

**Table 2.** Blood Flow Measurement at Plantar Surface after Ischemic Surgery

| Timing after the surgery | Perfusion unit (PU) at plantar surface: mean (SD) |           |               |
|--------------------------|---|-----------|---------------|
|                          | Sham  | Ischemia  | I/S ratio (%) |
| 3 h                      | 1,000 (48)  | 90 (25)** | 8.9 (2)       |
| 1 day                    | 844 (175)   | 82 (24)*  | 10 (3)        |
| 3 days                   | 803 (360)   | 116 (34)  | 15 (3)        |

Significantly different from the sham group; \*:  $p < 0.05$ , \*\*:  $p < 0.01$  (*t*-test). SD: standard deviation, I/S: ischemia/sham.

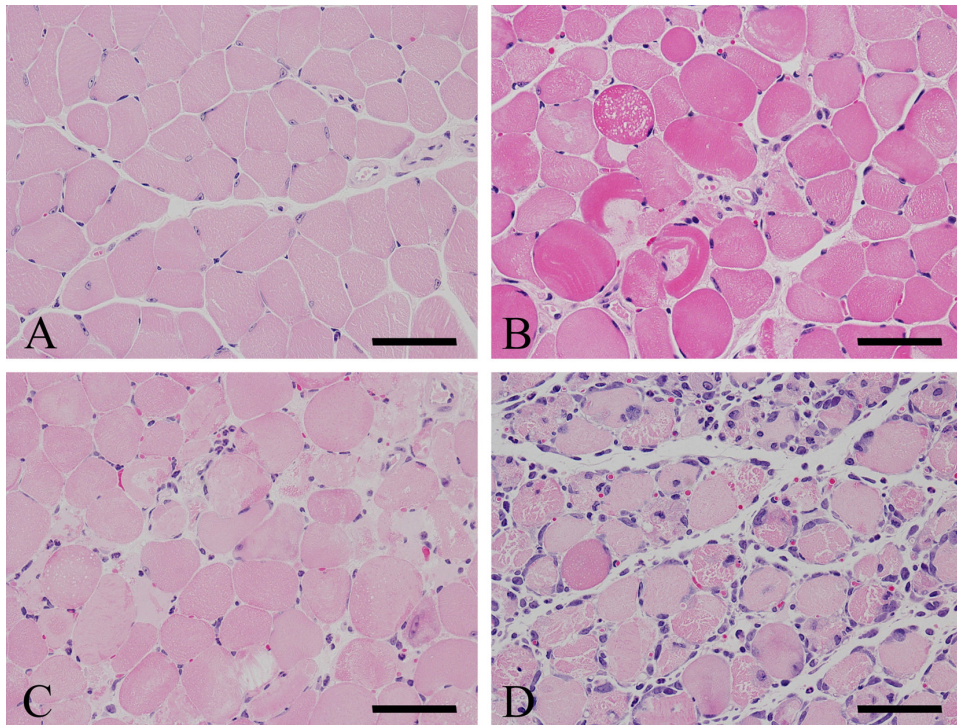


**Fig. 1.** Histological features of soleus in a non-ischemic hindlimb (A), and in ischemic hindlimbs 3 h (B), 1 d (C) and 3 d (D) after artery ligation. Necrosis/degeneration of muscle fiber was noted in more than half of the area in the ischemic hindlimb at 3 h. Infiltration of neutrophils and macrophages were observed in the interstitial tissue consistent with the necrotic area from 1 d after the artery ligation. Necrotic fibers were sporadically surrounded by myoblasts 3 d after the artery ligation, demonstrating regeneration. Scale bars = 100  $\mu$ m.

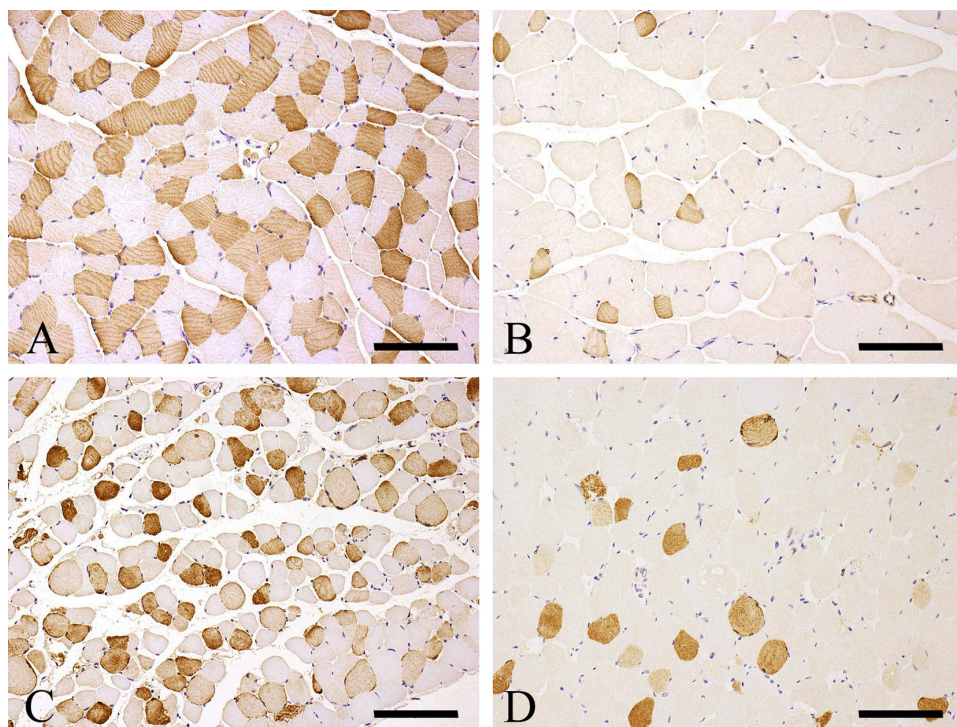


**Fig. 2.** Immunohistochemistry (IHC) of sarcoplasmic/endoplasmic reticulum calcium ATPase 2 (SERCA2). In the non-ischemic hindlimb, one third of muscle fibers in the soleus (A) and only a few fibers in the gastrocnemius (B) showed positive. These distributions in the ischemic hindlimbs were comparable to the non-ischemic hindlimb (C: soleus; D: gastrocnemius). IHC for slow troponin I showed similar histological distribution. Scale bars = 200  $\mu$ m.

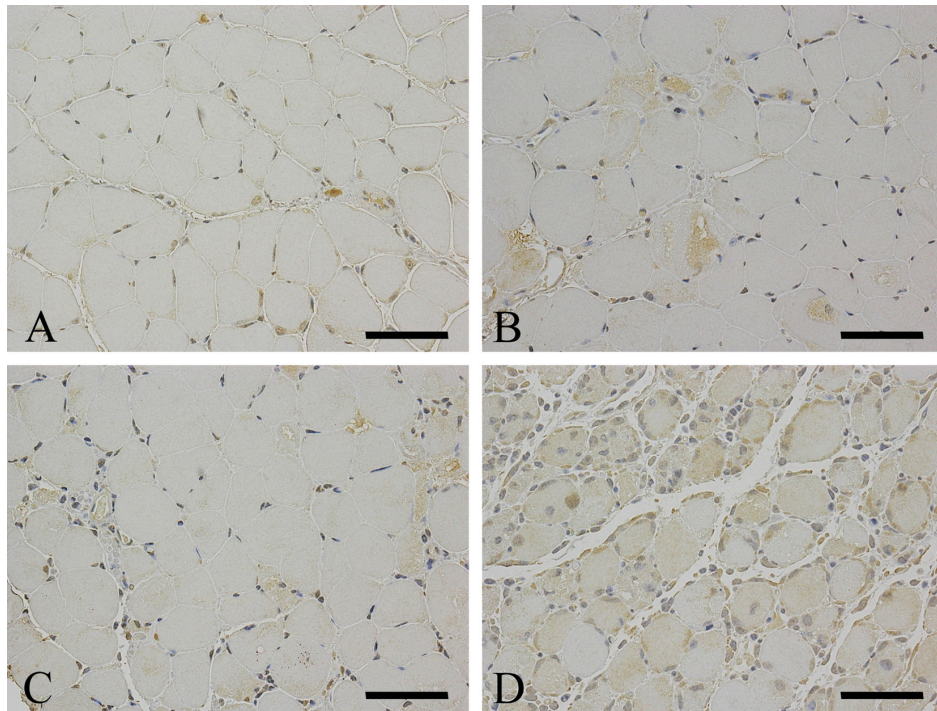


**Fig. 3.** Immunohistochemistry of hypoxia inducible factor-1 $\alpha$  (HIF-1 $\alpha$ ) in a non-ischemic hindlimb (A), and in ischemic hindlimbs 3 h (B), 1 d (C) and 3 d (D) after artery ligation. No positive reaction was observed in the non-ischemic hindlimb. In the ischemic hindlimbs, a few necrotic muscle fibers and infiltrative cells showed a positive signal following artery ligation. The magnitude of the positive signal was prominent in macrophages and regenerative myoblasts 3 d after the artery ligation. The positive signals were mainly observed in the cytoplasm, and partly in the nuclei of myoblasts. Scale bars = 100  $\mu$ m.

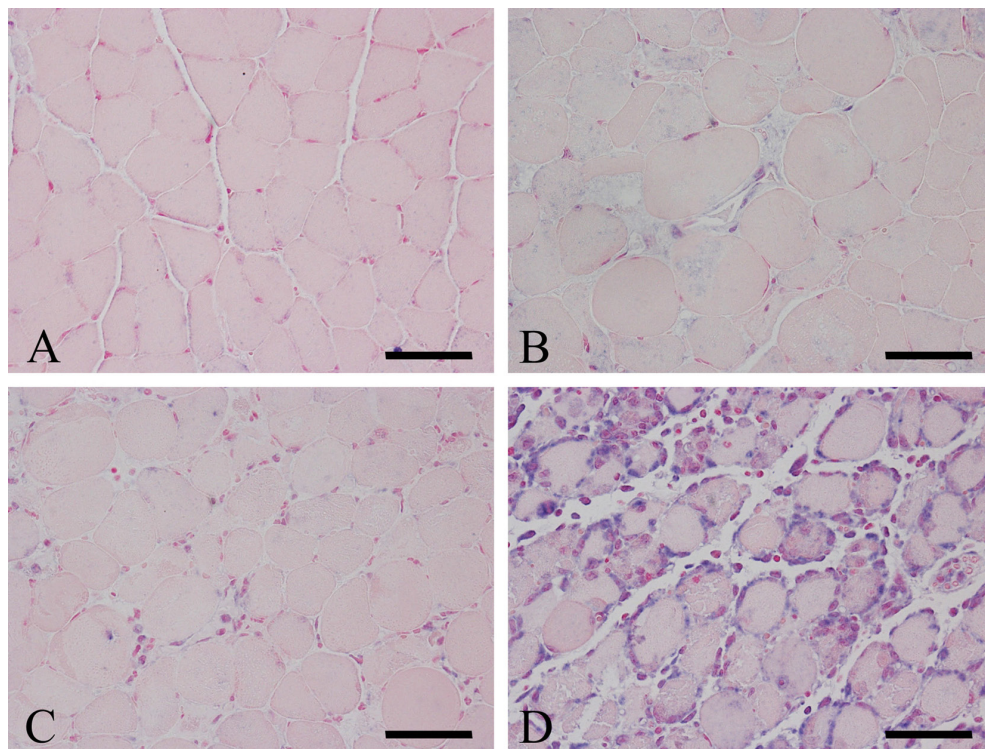


**Fig. 4.** *In situ* hybridization of microRNA (miR)-210 in a non-ischemic hindlimb (A), and in ischemic hindlimbs 3 h (B), 1 d (C) and 3 d (D) after artery ligation. No positive signal was observed in the non-ischemic hindlimb. In the ischemic hindlimbs, a few necrotic muscle fibers and infiltrative cells showed positive signals after the artery ligation. The magnitude of the positive signals was prominent in macrophages and regenerative myoblasts 3 d after the artery ligation. The positive signal was mainly observed in the cytoplasm. The histological distribution of miR-210 was similar to that of hypoxia inducible factor-1 $\alpha$  (HIF-1 $\alpha$ ) in Fig. 3. Scale bars = 100  $\mu$ m.

**Table 3.** Relative Expression of miR-210 to miR-191-5p

| Timing after the surgery | Soleus: mean (SD) |             |               | Gastrocnemius: mean (SD) |               |               |
|--------------------------|-------------------|-------------|---------------|--------------------------|---------------|---------------|
|                          | Sham              | Ischemia    | I/S ratio (%) | Sham                     | Ischemia      | I/S ratio (%) |
| 3 h                      | 0.48 (0.18)       | 0.42 (0.18) | 107 (86)      | 0.072 (0.020)            | 0.070 (0.024) | 99 (39)       |
| 1 day                    | 0.88 (0.11)       | 0.68 (0.03) | 79 (11)       | 0.051 (0.009)            | 0.091 (0.054) | 187 (123)     |
| 3 days                   | 0.48 (0.07)       | 1.06 (0.67) | 228 (145)     | 0.072 (0.044)            | 0.110 (0.037) | 183 (81)      |

No significantly difference from the sham, SD: standard deviation, I/S: ischemia/sham, miR: microRNA.

To induce ischemia, we used the femoral artery ligation model, and ischemia was continuously monitored until 3 d after the surgery by measuring the blood flow at the plantar surface using laser Doppler imaging. In the histopathology, necrosis/degeneration of muscle fiber was noted from 3 h, accompanied by infiltration of neutrophils/macrophages and muscular regeneration at 1 d and 3 d after the surgery, respectively. These histopathological effects were more severe in sites where type I muscle fibers are predominantly located, such as the soleus, which are susceptible to hypoxia due to their high oxygen requirements<sup>15</sup>. In addition, histopathological findings in gastrocnemius were also mainly distributed where type I muscles are located.

In the ischemic model using femoral artery ligation, massive muscular degeneration/necrosis was induced and the histological distributions of HIF-1 $\alpha$  and miR-210 were sparse in the muscle fibers during the acute phase, such as at 3 h and 1 d after the surgery. Zaccagnini et al. proposed that miR-210 may have protective effects on skeletal muscle under a peripheral ischemic model with femoral artery removal through the inhibition of reactive oxygen species formation by switching from phosphorylation to glycolysis, and our observation that the inhibition of miR-210 exacerbated the acute phase muscular necrosis in the gastrocnemius from 1 d after the surgery fits with this concept<sup>13</sup>. Although the histopathological distribution of miR-210 was not evaluated by Zaccagnini et al., our study revealed no histological miR-210 expression in intact muscle fibers in the ischemic hindlimb. Therefore, our result that histological miR-210 expression or cell infiltration was not observed in the intact area might imply that low miR-210 expression at the physiological level in intact tissue is important for the protection of injury from ischemia, especially in the early phase.

In contrast, muscular regeneration was observed 3 d after the ischemic surgery, and the histological expression of both HIF-1 $\alpha$  and miR-210 was noted in macrophages and myoblasts, especially in the soleus, where pathological changes were more severe. It has been reported that miR-210 expression in the myoblasts increases with a HIF-1 $\alpha$ -dependent mechanism and has a cytoprotective function against mitochondrial dysfunction and oxidative stress, although miR-210 is not necessary for myogenic differentiation<sup>16</sup>. In addition, miR-210 in macrophages seems to have an anti-inflammatory effect via inhibition of NF- $\kappa$ B<sup>17</sup>. Zaccagnini et al. reported that the expression of miR-210 was increased from 3 d after the ischemic surgery and was highest at 7 d after surgery, which is considered the regenerative

phase<sup>13</sup>. Therefore, the expression of miR-210 in myoblasts and macrophages seen in our results was considered to play an important role in outcomes such as regeneration and anti-inflammatory effects following hypoxia-induced necrosis.

HIF-1 $\alpha$  is widely used as an immunohistochemical marker for the detection of hypoxia<sup>1, 2</sup>. However, HIF-1 $\alpha$  expression in the nuclei is sometimes immunohistochemically detected in various tissues, including skeletal muscle, even under normoxic conditions<sup>2</sup>, which may imply that we cannot detect hypoxia using only IHC for HIF-1 $\alpha$ . In addition, the expression of HIF-1 $\alpha$  in nuclei was limited, although its expression in cytoplasm was relatively clear in our immunohistochemical procedure. Since we clearly identified histological miR-210 expression in the ischemic lesion, especially in the regenerative phase, with a tendency of increased tissue expression with qPCR, ISH for miR-210 could be used as a supplemental method to HIF-1 $\alpha$  staining for the detection of hypoxia. However, care must be taken when using these histological markers, because we could not clearly detect HIF-1 $\alpha$  or miR-210 expression in the acute phases, because HIF-1 $\alpha$  can be induced not only in hypoxia but also in other mechanisms such as oxidative or mechanical stresses<sup>18</sup>, and because a negative regulation of HIF-1 $\alpha$  by miR-210 exists<sup>19</sup>.

### Conclusion

We demonstrated that miR-210 is expressed in myoblasts and macrophages in the regenerative phase rather than the acute phase under hypoxic conditions using a peripheral ischemic model, which indicates that it plays pathophysiological roles in regeneration and anti-inflammatory effects. ISH for miR-210 has potential as a supplemental method to HIF-1 $\alpha$  staining for the detection of hypoxia, with careful consideration of its pathological significance.

**Disclosure of Potential Conflicts of Interest:** The authors declare that there are no conflicts of interest associated with this manuscript.

**Acknowledgment:** The authors would like to thank Dr. Yoko Hara and Ms. Yumiko Miyamoto for their support during this work.

## References

1. Chan YC, Banerjee J, Choi SY, and Sen CK. miR-210: the master hypoxamir. *Microcirculation*. **19**: 215–223. 2012. [[Medline](#)] [[CrossRef](#)]
2. Stroka DM, Burkhardt T, Desbaillets I, Wenger RH, Neil DA, Bauer C, Gassmann M, and Candinas D. HIF-1 is expressed in normoxic tissue and displays an organ-specific regulation under systemic hypoxia. *FASEB J*. **15**: 2445–2453. 2001. [[Medline](#)] [[CrossRef](#)]
3. Smith TG, Robbins PA, and Ratcliffe PJ. The human side of hypoxia-inducible factor. *Br J Haematol*. **141**: 325–334. 2008. [[Medline](#)] [[CrossRef](#)]
4. Devlin C, Greco S, Martelli F, and Ivan M. miR-210: More than a silent player in hypoxia. *IUBMB Life*. **63**: 94–100. 2011. [[Medline](#)]
5. Lou YL, Guo F, Liu F, Gao FL, Zhang PQ, Niu X, Guo SC, Yin JH, Wang Y, and Deng ZF. miR-210 activates notch signaling pathway in angiogenesis induced by cerebral ischemia. *Mol Cell Biochem*. **370**: 45–51. 2012. [[Medline](#)] [[CrossRef](#)]
6. Chang KP, and Lai CS. Micro-RNA profiling as biomarkers in flap ischemia-reperfusion injury. *Microsurgery*. **32**: 642–648. 2012. [[Medline](#)] [[CrossRef](#)]
7. Biswas S, Roy S, Banerjee J, Hussain SR, Khanna S, Meenakshisundaram G, Kuppusamy P, Friedman A, and Sen CK. Hypoxia inducible microRNA 210 attenuates keratinocyte proliferation and impairs closure in a murine model of ischemic wounds. *Proc Natl Acad Sci USA*. **107**: 6976–6981. 2010. [[Medline](#)] [[CrossRef](#)]
8. Armitage P, Berry G, and Matthews JNS. *Statistical methods in medical research*. John Wiley & Sons, 2008.
9. Usman MA, Nakasa T, Shoji T, Kato T, Kawanishi Y, Hamanishi M, Kamei N, and Ochi M. The effect of administration of double stranded MicroRNA-210 on acceleration of Achilles tendon healing in a rat model. *J Orthop Sci*. **20**: 538–546. 2015. [[Medline](#)] [[CrossRef](#)]
10. Ujigo S, Kamei N, Hadoush H, Fujioka Y, Miyaki S, Nakasa T, Tanaka N, Nakanishi K, Eguchi A, Sunagawa T, and Ochi M. Administration of microRNA-210 promotes spinal cord regeneration in mice. *Spine*. **39**: 1099–1107. 2014. [[Medline](#)] [[CrossRef](#)]
11. Kawanishi Y, Nakasa T, Shoji T, Hamanishi M, Shimizu R, Kamei N, Usman MA, and Ochi M. Intra-articular injection of synthetic microRNA-210 accelerates avascular meniscal healing in rat medial meniscal injured model. *Arthritis Res Ther*. **16**: 488. 2014. [[Medline](#)] [[CrossRef](#)]
12. Shoji T, Nakasa T, Yamasaki K, Kodama A, Miyaki S, Nimoto T, Okuhara A, Kamei N, Adachi N, and Ochi M. The effect of intra-articular injection of microRNA-210 on ligament healing in a rat model. *Am J Sports Med*. **40**: 2470–2478. 2012. [[Medline](#)] [[CrossRef](#)]
13. Zaccagnini G, Maimone B, Di Stefano V, Fasanaro P, Greco S, Perfetti A, Capogrossi MC, Gaetano C, and Martelli F. Hypoxia-induced miR-210 modulates tissue response to acute peripheral ischemia. *Antioxid Redox Signal*. **21**: 1177–1188. 2014. [[Medline](#)] [[CrossRef](#)]
14. Diao H, Liu B, Shi Y, Song C, Guo Z, Liu N, Song X, Lu Y, Lin X, and Li Z. MicroRNA-210 alleviates oxidative stress-associated cardiomyocyte apoptosis by regulating BNIP3. *Biosci Biotechnol Biochem*. **81**: 1712–1720. 2017. [[Medline](#)] [[CrossRef](#)]
15. Corsi A, Granata AL, and Hudlicka O. Effect of activity on performance and morphology in ischaemic rat slow muscles. *J Exp Biol*. **152**: 265–279. 1990. [[Medline](#)]
16. Cicchillitti L, Di Stefano V, Isaia E, Crimaldi L, Fasanaro P, Ambrosino V, Antonini A, Capogrossi MC, Gaetano C, Piaggio G, and Martelli F. Hypoxia-inducible factor 1- $\alpha$  induces miR-210 in normoxic differentiating myoblasts. *J Biol Chem*. **287**: 44761–44771. 2012. [[Medline](#)] [[CrossRef](#)]
17. Qi J, Qiao Y, Wang P, Li S, Zhao W, and Gao C. microRNA-210 negatively regulates LPS-induced production of proinflammatory cytokines by targeting NF- $\kappa$ B1 in murine macrophages. *FEBS Lett*. **586**: 1201–1207. 2012. [[Medline](#)] [[CrossRef](#)]
18. Chun YS, Kim MS, and Park JW. Oxygen-dependent and -independent regulation of HIF-1 $\alpha$ . *J Korean Med Sci*. **17**: 581–588. 2002. [[Medline](#)] [[CrossRef](#)]
19. Wang H, Flach H, Onizawa M, Wei L, McManus MT, and Weiss A. Negative regulation of Hif1 $\alpha$  expression and TH17 differentiation by the hypoxia-regulated microRNA miR-210. *Nat Immunol*. **15**: 393–401. 2014. [[Medline](#)] [[CrossRef](#)]